Original Article

The Growth of A549 Cell Line is Inhibited by Pemetrexed Through Up-regulation of hsa-MiR-320a Expression

Akbar Ghorbani Alvanegh[1], Hadi Esmaeili Gouvarchin Ghaleh[2], Shahla Mohammad Ganji[1]

[1]Department of Medical Biotechnology, National Institute of Genetic Engineering and Biotechnology (NIGEB), Tehran, Iran, [2]Applied Virology Research Center, Baqiyatallah University of Medical Sciences, Tehran, Iran

Abstract

Background: Lung cancer deaths are increasing worldwide and the most common form of lung cancer treatment is chemotherapy. Pemetrexed (PMX) has been shown to be effective as a second-line treatment for advanced patients. Drugs can alter the expression of MicroRNAs, and MicroRNAs also can either enhance or reduce the drug's effectiveness and this is a two-way relationship. *Hsa-MiR-320a* is known to play a crucial role in the lung cancer. This study aims to investigate the expression of *hsa-MiR-320a* in lung cancer cells after treatment with PMX.

Materials and Methods: A549 cells were cultured and treated with varying concentrations of PMX. Various parameters were measured, including cell viability, reactive oxygen species (ROS) production, lactate dehydrogenase (LDH) release, apoptosis assay, caspase 3 and 7 enzyme activity, and scratch assay. Additionally, gene expression profiles of *hsa-MiR-320a*, *VDAC1*, *STAT3*, *BAX*, and *BCL2* were evaluated.

Results: PMX reduced the viability and increased apoptosis. After 48 h, ROS production was 3.366-fold higher than in control cells and the LDH release rate was increased by 39%. PMX also up-regulated the expression of *hsa-MiR-320a* by about 12-fold change.

Conclusion: Changes in the expression of MicroRNAs occur after chemotherapy, and these changes play a crucial role in regulating the growth of cancer cells. Identifying these MicroRNAs can be helpful in predicting the efficacy of the chemotherapy or introducing it as combination therapy. Our research has been shown that *hsa-MiR-320a* can serve as a biomarker of PMX efficacy and also has the potential to be used in combination therapy.

Keywords: Apoptosis, lactate dehydrogenase, lung cancer, MicroRNAs, pemetrexed, reactive oxygen species

Address for correspondence: Dr. Shahla Mohammad Ganji, Department of Medical Biotechnology, National Institute of Genetic Engineering and Biotechnology (NIGEB), Tehran, Iran.
E-mail: shahlamg@yahoo.com, shahla@nigeb.ac.ir
Submitted: 29-Nov-2023; **Revised:** 18-Jan-2024; **Accepted:** 20-Jan-2024; **Published:** 29-Jul-2024

Introduction

Lung cancer occurs when cells in lung tissue grow uncontrollably. Lung cancer is one of the most common types of cancer affecting about 2.2 million people each year, and resulting in 1.8 million deaths.[1] There are two main types of lung cancer: small cell lung cancer (SCLC) and non-small cell lung cancer (NSCLC), with NSCLC being the most common, accounting for 85–90% of all cases.[2] Metastasis, the spread of cancer from its original location to other parts of the body, is the primary cause of death among individuals with lung cancer.[3] Treatment options, such as radiotherapy, chemotherapy, and surgery, are available depending on the patient's condition.[4]

Pemetrexed (PMX) is a highly effective chemotherapy agent used to treat non-squamous NSCLC that has metastasized. The US FDA approved its use as an infusion medicine on July 2, 2005.[5] PMX is capable of binding strongly with the folate receptor and can enter cells through the reduced folate transporter, just like folic acid. PMX and methotrexate share a similar mechanism of cell entry. Once inside the cells, PMX

Access this article online

Quick Response Code:

Website: www.advbiores.net

DOI: 10.4103/abr.abr_483_23

How to cite this article: Ghorbani Alvanegh A, Esmaeili Gouvarchin Ghaleh H, Mohammad Ganji S. The growth of A549 cell line is inhibited by pemetrexed through up-regulation of hsa-MiR-320a expression. Adv Biomed Res 2024;13:50.

is transformed into active pentaglutamate by the action of polyglutamate synthase (FPGS).[6]

MicroRNAs are being considered as potential biomarkers to predict efficacy of drugs.[7] MicroRNAs are responsible for regulating gene expression and translation by binding to the 3′ untranslated region (3′ UTR) of messenger RNA (mRNA).[8] There are two main types of MicroRNAs with significant roles in cells: tumor suppressors and oncogenes. Chemotherapy drugs can be effective either by deregulation or modulating MicroRNAs.[9]

According to researches, *hsa-MiR-320a* plays a crucial role in the development of certain types of tumors. It works as a tumor suppressor by decreasing the levels of Rab11a expression and enhancing the activity of the AKT signaling pathway.[10] *Hsa-MiR-320a* inhibits lung cancer cell growth, metastasis and enhances radiation-induced cell death by directly controlling *STAT3* signaling.[11] *Hsa-MiR-320*a interacts with the 3′ UTR of IGF-1R, inhibiting NSCLC cell development, proliferation, and invasion.[12] These findings suggest that *hsa-MiR-320a* could be a promising gene therapy strategy for people with lung cancer.[13] This study aims to investigate the expression of hsa-MiR-320a in lung cancer cells after treatment with PMX and also to investigate the role of PMX as a mediator between drugs and genes.

Materials and Methods

Cell line culture

The Institute Pasteur in Tehran provided the A549 human lung cancer cell line. The cells were cultured in DMEM (Gibco, USA) with 10% FBS (Bio-idea, Iran) and 1% penicillin-streptomycin (Bio-idea, Iran) and incubated at 37°C with 98% humidity and 5% CO2.

MTT assay

Cell viability was assessed in A549 cells using a colorimetric assay. Twelve doses of PMX (1, 2, 3,…, and 12 µM) were given for 24 and 48 h. viable cells convert MTT (Sigma-Aldrich, USA) into purple formazan crystals. After incubation, the formazan crystals were dissolved and the color intensity was measured with an ELISA plate reader at 570 nm.[14] Cell viability was measured at 100% with no intervention and at varying doses using the following formula:

$$\text{cell viability}(\%) = \frac{\text{OD of 570 nm of treated cells}}{\text{OD of 570 nm of control cells}} \times 100$$

Lactate dehydrogenase assay (LDH)

To evaluate the cytotoxicity of PMX, the release of LDH into the culture medium as an indicator of cell death was monitored. According to manufacturer's guideline (Kiazist, Iran) 10^4 cells/well were seeded into a 96-well plate with 200 µl of volume per well. After overnight incubation under proper cell growth conditions, 20 µl of PMX (IC_{50} dose) was added to each well. Following 24 and 48 h of incubation, 20 µl of Permi solution was added to the positive control wells and incubated for an additional hour at room temperature. Then 150µl of the solution was centrifuged at 400g for 5 min and 50 µl of the supernatant to was an equal proportion of buffer and substrate solution. The mixture was incubated at 37°C for 30 min in the dark and examined the samples using an ELISA plate reader at 570 nm. Finally, the cytotoxicity percentage was calculated using the following equation.[15]

$$\text{Cytotoxicity}(\%) = \frac{\text{Treated with PMX absorption} - \text{No treated absorption}}{\text{Treated with permi solution absorption} - \text{No treated absorption}} \times 100$$

ROS production assay

Cells were cultured in a 96-well black plate at a density of 10^4 cells per well to measure ROS production. After overnight incubation, cells were treated with PMX (IC_{50} dose). 100 µl of 2', 7'-dichlorofluorescein diacetate solution was added to each well and incubated for 45 min. The fluorescence intensity was measured using a microplate reader at 528/485 nm. Results were presented as fold change compared to untreated cells.[16]

Determination of caspase 3,7 activity

Cell lysis activity was evaluated using the caspase 3, 7 activity kit (Kiazist, Iran). PMX-treated and negative control cells were washed with cold PBS, trypsinized, and mixed with lysing buffer for 20 min at 4°C. After centrifugation at 12000 g for 15 min at 4°C, the caspase buffer, DTT, and substrate mix were added to 50 µl of the sample in 55.5 µl. Incubation was done for 2 h at 37°C followed by absorbance measurement at 405 nm using an ELISA plate reader. Results were expressed as units/mg protein after standardizing with the Bradford assay.[17]

Apoptosis assay by fluorescent dyes

The study investigated the impact of PMX on the death of A549 cells by using double labeling with AO/EtBr (Sigma-Aldrich, USA). A 24-well plate containing 10^4 uniformly dispersed cells was used for the experiment. The cells were incubated overnight, followed by exposure to PMX for 24 or 48 h. The wells were rinsed twice with PBS, and then a 250 µL solution of AO/EtBr (consisting of 5 µg/mL AO and 5 µg/mL EtBr in PBS) was added. The cells were allowed to incubate for 2 min, following which the supernatant was removed. The next step involved observing cell apoptosis under a fluorescent microscope to gain a better understanding of the cellular process.[18]

Apoptosis assay by flow cytometry

This study used flow cytometry and Annexin V/FITC/PI (BD Biosciences, USA) labeling to investigate cellular apoptosis. Cells were treated with PMX for 24 and 48 h, then washed, trypsinized, and collected in PBS. After staining with the Annexin V/FITC/PI apoptosis detection kit, the BD FACSCalibur flow cytometer was used to analyze the data, which was processed using FlowJo.[19]

Scratch assay

To evaluate the two-dimensional cell migration, the Scratch assay was conducted as follows: 2×10^5 A549 cells were seeded in a 6-well plate and cultured under optimal cell growth conditions for 24 h. Next, a scratch line was made in the middle of the well using the tip of the yellow sampler. The well was gently washed with PBS to remove any unattached cells. The cells were then treated with PMX and imaged at 0, 24, and 48 h using an inverted microscope at 100X magnification. To count moving cells and normalize image fields, ImageJ version 1.52 was used.[18]

RNA extraction

RNA was extracted from 10^6 cells by adding 1 mL of RNX-plus ™ (Sinaclon, Iran). After incubation, severe shaking was done with 250 µL of chloroform. The mixture was centrifuged, and the aqueous phase was transferred to a fresh microtube and 500 µL isopropanol was added. Following this, the pellet was dissolved in RNase-free water and RNase-free DNase I (Sinaclon, Iran) was used to remove any potential genomic DNA. The resulting RNA was quantified using the NanoDrop.[20]

cDNA Synthesis

Complementary DNA (cDNA) was syntheses using cDNA Synthesis Kit (addbio-Korea). For the synthesis of coding genes cDNA, 1 µg of total RNA was mixed with 1µl of oligo dT, 2µl of dNTPs, 1µl of RT enzyme, and 10 µl of reaction buffer. The solution was then diluted with DEPC water to a final volume of 20 µl. For the synthesis of hsa-miR-320a and U48 cDNA, 1 µl of specific stem-loop RT primer was used instead of oligo dT. Reaction was incubated at 25°C for 10 min, 50°C for 60 min, and 80°C for 5 min. Finally, cDNA was stored at -70°C.[21]

Real-time PCR

For real-time PCR, a mixture was prepared using Prime Q-Master Mix with SYBR Green I (Parstous, Iran) along with forward and reverse primers, and cDNA. U48 and GAPDH were used as internal housekeeping controls for *hsa-MiR-320a* and coding genes, respectively. The coding genes selected were *VDAC1, STAT3, BAX*, and *BCL2*. The temperature protocol used for amplification was a cycle at 95°C for 15 min, followed by 40 cycles of 15 s at 95°C, 15 s at the annealing temperature, and 10 s at 72°C. Duplicate PCR was used in all real-time PCR. NORT and NTC were used as negative control for genomic DNA and environmental cDNA contamination, respectively.[22] Primer sequences of non-coding and coding genes are presented in Tables 1 and 2.

Ethics and the approval of the ethics committee of the National Institute of Genetic Engineering and Biotechnology (NIGEB).

Statistical analysis

This research uses GraphPad Prism program version 8.2.1.(441, ©1992-2019 GraphPad Software, Inc). The data are presented as mean values and SDs from three testing. Two-Way ANOVA of variance was used to compare two and multiple groups. The P-value of 0.05 revealed a statistically significant difference in analysis outcomes.

Results

Cytotoxicity assay

The MTT test was used to measure the cytotoxic effect of PMX on the A549 cells after 24 and 48 h of exposure. Figure 1a indicates that the A549 cell line responds significantly to PMX, with the strength of this response depending on the concentration of the drug. The IC_{50}, which is the concentration of PMX required to cause a 50% decrease in cell viability,

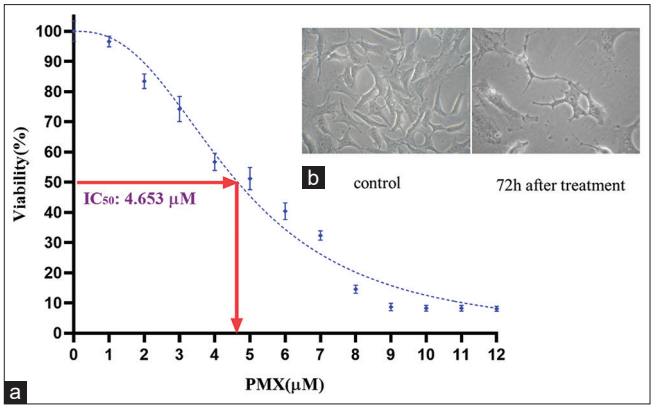

Figure 1: The effectiveness of PMX in inhibiting cell growth was evaluated using MTT assays. After 24 h of treatment, the concentration of PMX that resulted in 50 percent cell survival was found to be 4.653 (a). The morphology of A549 cell lines was imaged after 72 h of exposure to PMX in comparison with the control group, using microscopy with 400X magnification (b)

Table 1: Primer sequences of *hsa-MiR-320a* and *U48*

miRNA	Sequence	Primer sequence
hsa-MiR-320a-3p (MIMAT0000510)	AAAAGCUGGGUUGAGAGGGCGA	Stem-loop primer: GTCGTATCCAGTGCAGGGTCCGAGGTATTCGCACTGGATACGACTCGCCCT Forward primer: ACGCCGAAAAGCTGGGTTG Reverse primer: GTCGTATCCAGTGCAGGGT
U48 (NR_002745.1)	AGTGATGATGACCCC AGGTAACTCTTGAGTGT GTCGCTGATGCCA TCACCGCAGCGCTCTGACC	Stem-loop primer: GTCGTATCCAGTGCAGGGTCCGAGGTATTCGCACTGGATACGACGGTCAG Forward primer: CTCTGAGTGTGTCGCTGATGCC Reverse primer: CCAGTGCAGGGTCCGAGGTA

was found to be 4.653 μM and 1.861 μM after 24 and 48 h of treatment, respectively. After exposing the A549 cells to PMX for 72 h, we observed changes in their shape and proliferation [Figure 1b]. The cellular atrophy occurred due to changes in the shape of A549 cells.

LDH assay

There has been a significant increase in LDH activity observed after PMX treatment. In the A549 cell line, LDH activity rose by 14.33% ($P = 0.0002$) after 24 h of treatment, and by 39% ($P < 0.0001$) after 48 h of treatment. It is worth noting that the increase in LDH activity between the 24 and 48 h marks was statistically significant, with a rise of 24.67% ($P = 0.0001$) [Figure 2a].

ROS production

According to the results, PMX-treated cells produced significantly more ROS than the control cells. Specifically, after being exposed to PMX, the cells in A549 showed a significant increase in the production of ROS. After 24 h of treatment, the ROS production was 1.43 times higher than in control cells ($P = 0.0337$). Furthermore, after 48 h of treatment, the ROS production was 3.366-fold higher than in control cells ($P < 0.0001$). It is important to note that after 48 h of treatment, the ROS produced was found to be 2.342 times higher than after 24 h of treatment with PMX ($P < 0.0001$) [Figure 2b].

Effect of PMX on caspase 3, 7 activity

Caspase 3 and 7 activities in A549 cells increased significantly when exposed to PMX at the IC_{50} dose compared to the control group. After 24 h, caspase 3 and 7 activity was 3.284 times higher ($P < 0.0001$), and after 48 h, it increased 6.927-fold ($P < 0.0001$) compared to the control group. The 48 h PMX treatment also showed a 2.108-fold increase in caspase 3 and 7 activity compared to the 24 h treatment ($P < 0.0001$) [Figure 2c].

Apoptosis

To explore the role of PMX in apoptosis and necrosis, Annexin V-PE/PI staining was employed. Experiment A549 revealed that the use of PMX treatment led to a higher percentage of apoptotic cells compared to the control group. In the A549 cell line, after 24 h of treatment, the percentage of late apoptotic cells was found to be 14.4%, which remained constant at 48 h.

The percentage of necrosis cells was found to be 1.24%, and 28.5% after 24 and 48 h, respectively. Additionally, after 48 h of treatment with PMX, the percentage of living cells was almost 60% of the control cells (as shown in Figure 3a). The number of living cells almost doubled from the number in the control group. To observe apoptosis in PMX-treated cells, Acridine orange (AO) and ethidium bromide staining were used, which revealed clear differences in cellular morphology between the live cells and dead cells (as displayed in Figure 3b). Green cells with a normal nucleus shape indicated that AO dye the living cells. It is also noteworthy

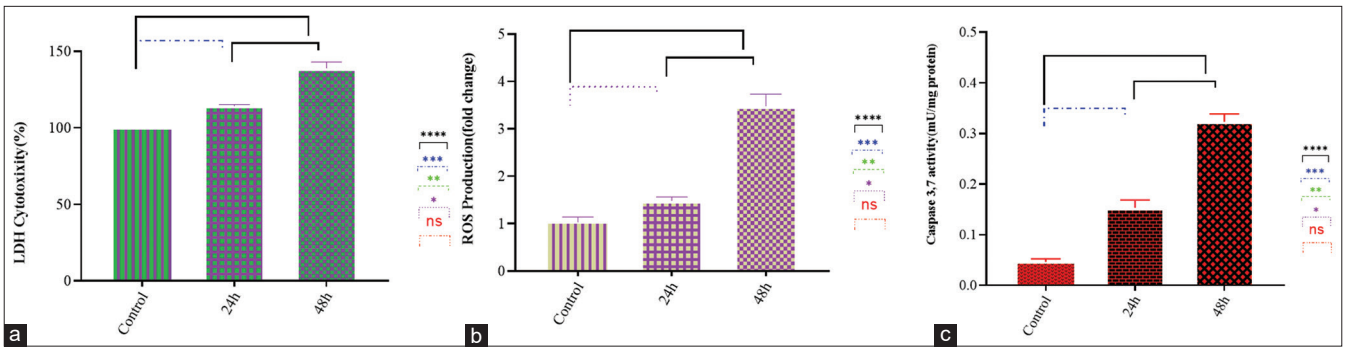

Figure 2: The effect of PMX treatment on LDH (a), ROS production (b), and caspase 3, 7 activity (c) of the A549 cell line. (*indicates Significance at the $P < 0.05$ level. ** indicates Significance at the $P < 0.01$ level. *** indicates Significance at the $P < 0.001$ level. **** indicates Significance at the $P < 0.0001$ level)

Table 2: Primer sequences of coding genes, annealing temperatures, and PCR product size

Accession number and Gene names		Forward or Reverse	Primer sequences (5`-3`)	Length (bp)	Annealing temp (°C)	Product size (bp)
NM_002046.7	*GAPDH*	F	GACAACTTTGGTATCGTGGAAGG	23	60	133
		R	AGGCAGGGATGATGTTCTGG	20		
NM_001291428.2	*BAX*	F	TTTCTGACGGCAACTTCAACTG	22	59	127
		R	TCCAATGTCCAGCCCATGA	19		
NM_000633.3	*BCL2*	F	TCATGTGTGTGGAGAGCGTC	20	59	257
		R	ACTTCACTTGTGGCCCAGAT	20		
NM_139276.3	*STAT3*	F	ATGCGGAGAAGCATCGTGAG	20	60	125
		R	CCTCCAATGCAGGCAATCTG	20		
NM_001401008.1	*VDAC1*	F	GTTTGGCGGCTCCATTTACC	20	59	161
		R	TCAGGCTGGAGTTGTTCACTT	21		

that apoptotic cells change color from yellow to light orange in the early stages of the process and then to a deeper orange to red in the late stages.

Scratch assay

We used a scratch assay to test the effect of PMX on cell migration on a 2D substrate (refer to Figure 3c). Results showed a significant difference ($P < 0.05$) in the number of migratory cells within the scratch gaps of tested cells.

Hsa-MiR-320a has a potential binding site on VDAC1 mRNA

It was analyzed whether miRNA molecules can bind to the 3′-UTRs of *VDAC1* and *STAT3* genes using TargetScan (www.targets.org) and RNA hybrid (https://bibiserv.cebitec.uni-bielefeld.de/rnahybrid) tools. This was done to identify possible miRNA targets on *VDAC1* and *STAT3*. The results, illustrated in Figure 4, indicate that *hsa-MiR-320a* can bind to a conserved site in the 3′-UTR of both the 8-mer (VDAC1) and the 7-mer (STAT3) of the human genome [Figure 4].

Real-time PCR

PMX increased the expression of *hsa-MiR-320a* by +12.338-fold change ($P < 0.05$) after 48 h of treatment. The RNA expression levels of *STAT3* and *VDAC1*, direct targets of *hsa-MiR-320a*, were lower in the PMX-treated A549 cells compared to the control. The RNA expression levels of *BAX* and *Bcl2*, indirect targets of *hsa-MiR-320a*, showed that treatment with PMX up-regulated *BAX* and down-regulated *Bcl2* ($P < 0.05$). [See Table 3, Figure 5a-d].

Discussion

In recent times, PMX has gained popularity as a chemotherapeutic drug for treating advanced NSCLC, and

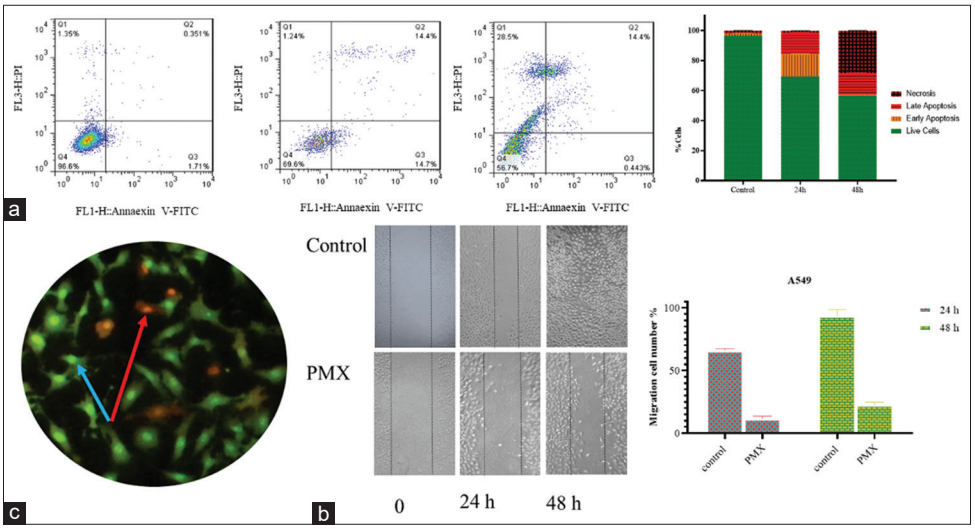

Figure 3: The study was evaluated cell death induction using an apoptosis assay with Annexin V-PE/PI and flow cytometry. Results were presented in graphs, quarters of Q1, Q2, Q3, and Q4 that represent dead cells, late apoptosis/necrosis, early apoptosis, and live cells, respectively (a). The study also performed Acridine orange (AO) and ethidium bromide staining on the A549 cell line, capturing images with fluorescent microscopy. The results were analyzed and represented using arrows, with blue indicating living cells, and red indicating apoptosis cells (b). To assess the effect of PMX on the mobility of the A549 cell line, a scratch assay was used. Images of scratched control cells and PMX-treated cells were taken at 0, 24, and 48 h after scratch creation with an objective magnification of 40X. The results were represented in graphs as the means ± SD ($P < 0.0001$) (c)

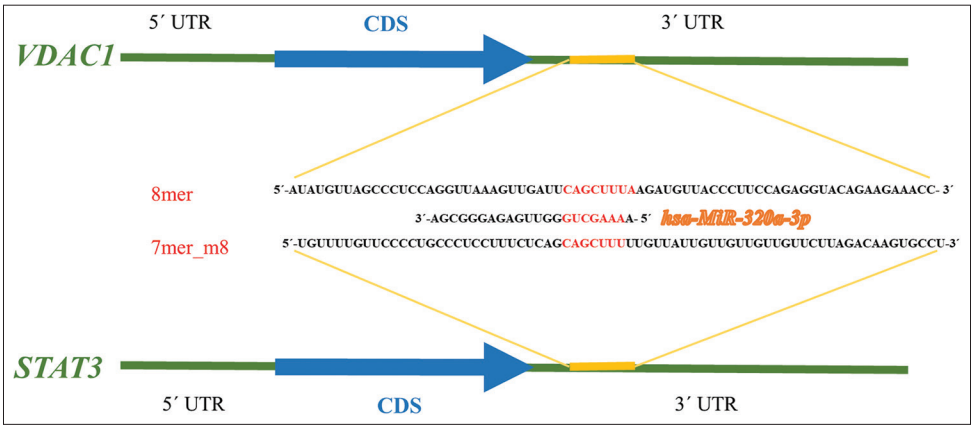

Figure 4: *hsa-MiR-320a* binding sites were analyzed in *VDAC1* mRNA 3′-UTR and *STAT3* using bioinformatics. A schematic diagram shows one target site in *VDAC1 (*8mer) and one target site in *STAT3 (*7mer-m8)

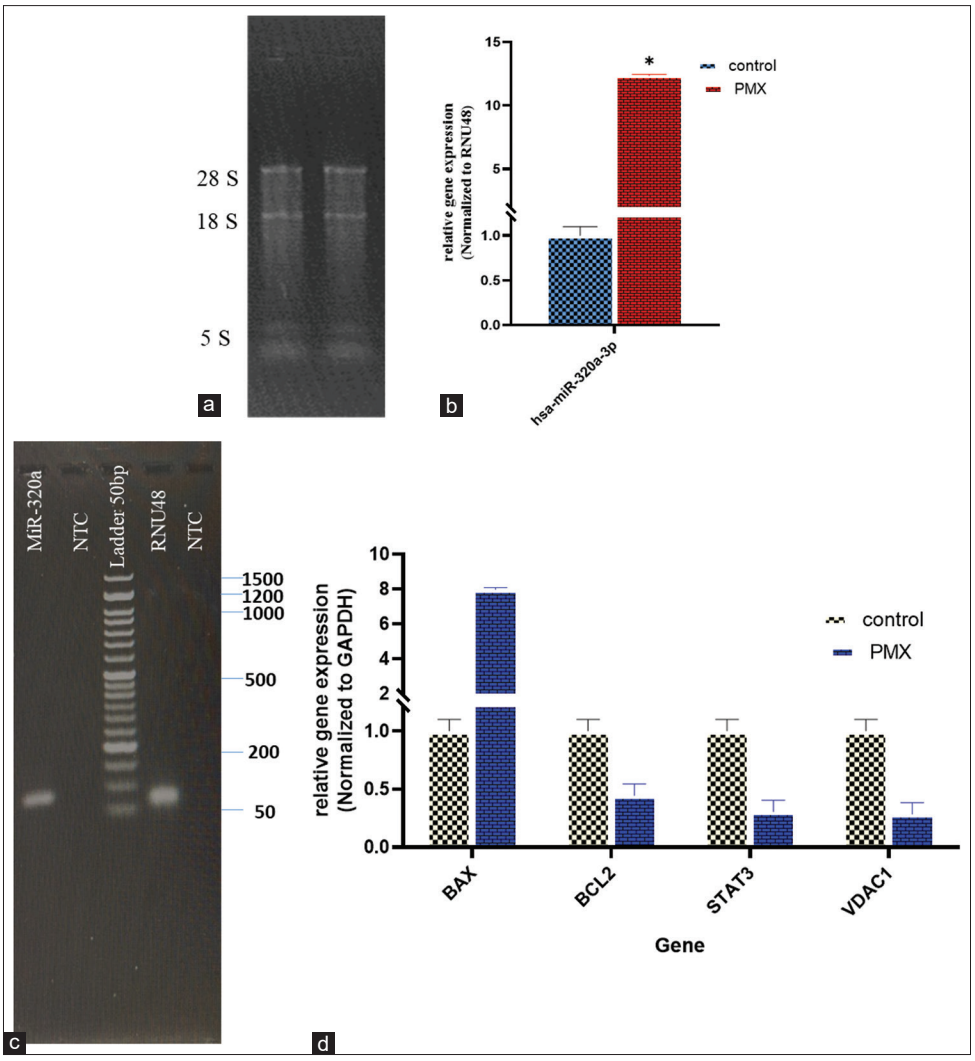

Figure 5: RNA extraction electrophoresis gel (1%) from A549 with and without PMX-treated after DNase I treatment (a). Relative expression of *hsa-MiR-320a* in PMX-treated A549 vs Control A549 that normalized to *RNU48*. Expression of *hsa-MiR-320a* was significantly up-regulated in PMX-treated A549 vs Control A549 (b). Electrophoresis gel (2%) for *hsa-MiR-320*a and to *RNU48* (c). Relative expression of *BAX, BCL2, STAT3*, and *VDAC* in PMX-treated A549 vs. Control A549 that normalized to *GAPDH*. Expression of *BAX* was significantly up-regulated in PMX-treated A549 vs. Control A549. Expression of *BCL2, STAT3* and *VDAC1* were significantly down-regulated in PMX-treated A549 vs Control A549 (d)

Table 3: *Hsa-MiR-320a* and genes expression profile

miRNA or genes	Fold change
hsa-MiR-320a-3p (MIMAT0000510)	(+) 12.338
BAX	(+) 7.972
BCL2	(-) 2.252
STAT3	(-) 3.289
VDAC1	(-) 3.353

it has been approved for use in the first, second, and third lines of treatment for NSCLC.[23] In recent years, MicroRNAs have been the focus of numerous studies because of their potential role in cancer, diagnosis, prognosis, and gene therapy. These post-transcriptional gene regulators can affect several biological activities, including drug resistance. Recent research has linked the deregulation of specific MicroRNAs to the development of treatment resistance in different cancers. By using miRNA mimics or antagomiRs, it has been demonstrated that these MicroRNAs can be controlled to modify regulatory networks and signaling cascades. This modification may serve as a therapeutic alternative to make cancer cells more responsive to chemotherapy.[24]

MicroRNAs can be used as biomarkers to predict the effectiveness of chemotherapy drugs. Koturbash, *et al*. (2015)[25] have identified several MicroRNAs, such as *hsa-MiR-200b* and *hsa-MiR-21*, which can indicate drug efficacy in lung cancer patients. Shi *et al*. (2016)[26] proposed *hsa-MiR-25*, *hsa-MiR-146, and hsa-MiR-210* as biomarkers for predicting PMX efficacy in lung adenocarcinoma. In addition, we introduce a new MicroRNA, called *hsa-MiR-320a*, which may be a potential gene therapy candidate with drugs.

It is currently uncertain which targets and processes are responsible for the anticancer properties of a certain chemical.

Mitochondria play a vital role in regulating cell growth and death, energy production, and the ROS production.[27] As a result, we investigated whether PMX induces apoptosis in cancerous mesothelioma and lung cells by increasing the production of ROS. Buqué *et al*. (2012)[28] discovered that PMX causes the production of ROS to increase by nearly two times in human melanoma cells. In lung cancer cells treated with PMX, increased levels of intracellular ROS and the accumulation of ROS production are major characteristics of DNA damage that triggers apoptosis. The highest caspase 3 activity was observed 72 h after PMX treatment.

Hwang *et al*. (2014)[29] evaluated the impact of PMX and simvastatin on the production of ROS in malignant mesothelioma and lung cancer cells. The results indicated that both drugs when used alone and in combination, increased the amount of ROS production. Additionally, PMX had the strongest effect on malignant mesothelioma cells. Furthermore, the combination of these drugs resulted in even greater production of ROS.

According to a study by Hwang *et al*. (2015),[30] PMX can trigger apoptosis in malignant mesothelioma and lung cancer cells by activating ROS production and inhibiting sirtuin 1. PMX causes ROS production, down-regulation of *SIRT1*, mitochondrial dysfunction, and cytochrome c release. This triggers caspase 9, which activates caspase 3 and cleaves *PARP*. Moreover, caspase 3, caspase 8, caspase 9, and *VDAC1* proteins increase in A549 cells treated with PMX.

LDH is found in the cytoplasm and is released into the extracellular medium when cells are damaged or dead, indicating cell membrane damage.[31] Ahamed (2013) investigated the leakage of LDH by inducing silica nanoparticles on the A549 cells. The results showed that the amount of LDH leakage in the culture medium of cells treated with nanoparticles at a concentration of 200 μg/ml was almost twice as much as in the culture medium of untreated cells. With cell membrane damage, LDH increased significantly in the cell culture medium.[32] Tang *et al*. (2015)[33] induced several concentrations of gold nanoparticles with the A549 cells. They showed that LDH leakage increases with increasing concentration. At a dose of 15 μg/ml, LDH concentration increased by 60% and cell viability decreased below 10%.

De-Ugarte *et al*. (2020)[34] transfected *hsa-MiR-320a* into human osteosarcoma cell lines using Lipofectamine to evaluate ROS production. They found that *hsa-MiR-320a* increased ROS production by 25%. The discovery of tumor biomarkers and therapeutic targets has led to new insights into the clinical treatment of lung cancer. Recent studies have shown that the expression of *hsa-MiR-320a* has a negative relationship with cancer cell growth, migration, and proliferation in call-3 and A549 cells.[35] Khandelwal A *et al*. (2021)[36] demonstrated that an increase in the expression of *hsa-MiR-320a* inhibited cell viability, cell proliferation, migration, and invasion. Their western blot result also indicated that the caspase 3 activity of A549 cells increased after *hsa-MiR-320a* transfection, which led to apoptosis.

Lv *et al*. (2017)[11] used Lipofectamine to transfer *hsa-MiR-320a* into A549/34R cells. Their study showed that *hsa-MiR-320a* significantly inhibits the growth of lung cancer cells compared to scram and negative control. This suppression is due to the down-regulation of *STAT3* expression, which in turn reduces the activity of downstream anti-apoptosis molecules like *Bcl2* and increases the activity of downstream apoptosis molecules like *CASP8, CASP9, CASP3*, and *BAX*. The study also found that overexpression of *hsa-MiR-320a* reduces migration. *VDAC1* is a key regulator of the exchange of ATP/ADP and respiratory control in the outer mitochondrial membrane. It controls the metabolic cross-talk between the mitochondria and the rest of the cell by mediating the flux of ions, nucleotides, Ca (2+), and other metabolites across the membrane. This is crucial for maintaining cell energy and metabolic homeostasis. Decreased *VDAC1* expression can suppress cell energy and metabolism.[37] Research by Zhang *et al*. (2016)[38] showed that suppressing *hsa-MiR-320a* expression increased NSCLC cells' proliferation and invasion due to the higher expression of *VDAC1*. *VDAC1* regulates mitochondrial apoptosis and controls the release and interaction of apoptosis-related proteins.

Our study showed there was a statistically significant rise in the percentage of apoptosis, ROS production, and LDH release, caspase 3, 7 activities after PMX treatment, and there was a marked drop in survival rate, and migration compared to the control group. These findings were consistent with the Buqué *et al.* (2012)[28].

As mentioned abo*ve Hsa-MiR-320a* regulates both direct and indirect target genes to achieve its biological effects, which include inducing apoptosis, blocking metastasis, and decreasing proliferation. Several direct and indirect target genes' expression levels were analyzed in this research. Our bioinformatics analysis showed that by up-regulation of *hsa-MiR-320a*, the gene expression of *VDA*C1 and *STAT3* decreases, and *in vitro* experiment results proved this.

As mentioned by Lv *et al.* (2017)[11] by down-regulation *STAT3*, the expression of *BAX* and *BCL2* up and down-regulated respectively. Our results were consistent with the results of Zhang *et al.* (2016)[38] and the up-regulation of *hsa-MiR-320a* had inversely related to the expression of *VDAC1*. Down-regulation of *VDAC1* may deregulate the flux of ions, Ca (2+), and other metabolites across the outer mitochondrial membrane and cause inhibition of cell proliferation.

Conclusion

The results of our experiment showed that when lung cancer cells treatment with PMX, *hsa-MiR320a* up-regulated. This up-regulation can be introduced it as biomarker to predict the effectiveness of treatment with PMX. Our findings also showed that *hsa-MiR-320a* acts as a tumor suppressor in lung cancer by regulating another genes such as *VDAC1* and *STAT3* and can potentially effective therapy option in combination with PMX.

Acknowledgment

Authors wish to thank the National Institute of Genetic Engineering and Biotechnology (NIGEB) for providing

equipment and approval for project number 838 and also appreciate NanoAlvand Company for providing the pemetrexed.

Financial support and sponsorship

This work is based upon research funder by Iran National Science Foundation (INSF) under project No. 4004225 and also was supported by grant No: biodc-35340-35342.2 of the Biotechnology Development Council of the Islamic Republic of Iran**.**

Conflicts of interest

There are no conflicts of interest.

References

1. Lahiri A, Maji A, Potdar PD, Singh N, Parikh P, Bisht B, *et al*. Lung cancer immunotherapy: Progress, pitfalls, and promises. Mol Cancer 2023;22:40.
2. Khan SR, Scheffler M, Soomar SM, Rashid YA, Moosajee M, Ahmad A, *et al*. Role of circulating-tumor DNA in the early-stage non-small cell lung carcinoma as a predictive biomarker. Pathol Res Pract 2023;245:154455.
3. Raczkowska J, Bielska A, Kręt owski A, Niemira M. Extracellular circulating miRNAs as potential non-invasive biomarkers in non-small cell lung cancer patients. Front Oncol 2023;13:1209299.
4. Lemjabbar-Alaoui H, Hassan OU, Yang YW, Buchanan P. Lung cancer: Biology and treatment options. Biochim Biophys Acta 2015;1856:189-210.
5. Cohen MH, Cortazar P, Justice R, Pazdur R. Approval summary: Pemetrexed maintenance therapy of advanced/metastatic nonsquamous, non-small cell lung cancer (NSCLC). Oncologist 2010;15:1352-8.
6. Kuo WT, Tu DG, Chiu LY, Sheu GT, Wu MF. High pemetrexed sensitivity of docetaxel-resistant A549 cells is mediated by TP53 status and downregulated thymidylate synthase. Oncol Rep 2017;38:2787-95.
7. Ding L, Wang R, Shen D, Cheng S, Wang H, Lu Z, *et al*. Role of noncoding RNA in drug resistance of prostate cancer. Cell Death Dis 2021;12:590.
8. O'Brien J, Hayder H, Zayed Y, Peng C. Overview of MicroRNA biogenesis, mechanisms of actions, and circulation. Front Endocrinol 2018;9:402.
9. Gamazon ER, Trendowski MR, Wen Y, Wing C, Delaney SM, Huh W, *et al*. Gene and MicroRNA perturbations of cellular response to pemetrexed implicate biological networks and enable imputation of response in lung adenocarcinoma. Sci Rep 2018;8:733.
10. Wang B, Yang Z, Wang H, Cao Z, Zhao Y, Gong C, *et al*. MicroRNA-320a inhibits proliferation and invasion of breast cancer cells by targeting RAB11A. Am J Cancer Res 2015;5:2719-29.
11. Lv Q, Hu JX, Li YJ, Xie N, Song DD, Zhao W, *et al*. Hsa-MiR-320a effectively suppresses lung adenocarcinoma cell proliferation and metastasis by regulating STAT3 signals. Cancer Biol Ther 2017;18:142-51.
12. Wang J, Shi C, Wang J, Cao L, Zhong L, Wang D. MicroRNA-320a is downregulated in non-small cell lung cancer and suppresses tumor cell growth and invasion by directly targeting insulin-like growth factor 1 receptor. Oncol Lett 2017;13:3247-52.
13. Liang Y, Li S, Tang L. MicroRNA 320, an anti-oncogene target miRNA for cancer therapy. Biomedicines 2021;9:591.
14. Pozzolini M, Scarfi S, Benatti U, Giovine M. Interference in MTT cell viability assay in activated macrophage cell line. Anal Biochem 2003;313:338-41.
15. Ghadaksaz A, Imani Fooladi AA, Mahmoodzadeh Hosseini H, Nejad Satari T, Amin M. ARA-linker-TGFαL3: A novel chimera protein to target breast cancer cells. Med Oncol 2021;38:96.
16. Daei S, Ziamajidi N, Abbasalipourkabir R, Khanaki K, Bahreini F. Anticancer effects of gold nanoparticles by inducing apoptosis in bladder cancer 5637 cells. Biol Trace Elem Res 2022;200:2673-83.
17. Daei S, Ziamajidi N, Abbasalipourkabir R, Aminzadeh Z, Vahabirad M. Silver nanoparticles exert apoptotic activity in bladder cancer 5637 cells through alteration of Bax/Bcl-2 genes expression. Chonnam Med J 2022;58:102-9.
18. Dodangeh F, Sadeghi Z, Maleki P, Raheb J. Long non-coding RNA SOX2-OT enhances cancer biological traits via sponging to tumor suppressor miR-122-3p and miR-194-5p in non-small cell lung carcinoma. Sci Rep 2023;13:12371.
19. Maleki P, Mowla SJ, Taheri M, Ghafouri-Fard S, Raheb J. The role of long intergenic non-coding RNA for kinase activation (LINK-A) as an oncogene in non-small cell lung carcinoma. Sci Rep 2021;11:4210.
20. Mousavi B, Hedayati MT, Teimoori-Toolabi L, Guillot J, Alizadeh A, Badali H. cyp51A gene silencing using RNA interference in azole-resistant Aspergillus fumigatus. Mycoses 2015;58:699-706.
21. Dara M, Habibi A, Azarpira N, Dianatpour M, Nejabat M, Khosravi A, *et al*. Novel RNA extraction method from human tears. Mol Biol Res Commun 2022;11:167-72.
22. Shamsabadi RM, Basafa S, Yarahmadi R, Goorani S, Khani M, Kamarehei M, *et al*. Elevated expression of NLRP1 and IPAF are related to oral pemphigus vulgaris pathogenesis. Inflammation 2015;38:205-8.
23. Tomasini P, Barlesi F, Mascaux C, Greillier L. Pemetrexed for advanced stage nonsquamous non-small cell lung cancer: Latest evidence about its extended use and outcomes. Ther Adv Med Oncol 2016;8:198-208.
24. Condrat CE, Thompson DC, Barbu MG, Bugnar OL, Boboc A, Cretoiu D, *et al*. miRNAs as biomarkers in disease: Latest findings regarding their role in diagnosis and prognosis. Cells 2020;9:276.
25. Koturbash I, Tolleson WH, Guo L, Yu D, Chen S, Hong H, *et al*. microRNAs as pharmacogenomic biomarkers for drug efficacy and drug safety assessment. Biomark Med 2015;9:1153-76.
26. Shi SB, Wang M, Tian J, Li R, Chang CX, Qi JL. MicroRNA 25, microRNA 145, and microRNA 210 as biomarkers for predicting the efficacy of maintenance treatment with pemetrexed in lung adenocarcinoma patients who are negative for epidermal growth factor receptor mutations or anaplastic lymphoma kinase translocations. Transl Res 2016;170:1-7.
27. Kim HR, Kim EJ, Yang SH, Jeong ET, Park C, Kim SJ, *et al*. Combination treatment with arsenic trioxide and sulindac augments their apoptotic potential in lung cancer cells through activation of caspase cascade and mitochondrial dysfunction. Int J Oncol 2006;28:1401-8.
28. Buqué A, Muhialdin JSh, Muñoz A, Calvo B, Carrera S, Aresti U, *et al*. Molecular mechanism implicated in Pemetrexed-induced apoptosis in human melanoma cells. Mol Cancer 2012;11:25.
29. Hwang KE, Kim YS, Hwang YR, Kwon SJ, Park DS, Cha BK, *et al*. Enhanced apoptosis by pemetrexed and simvastatin in malignant mesothelioma and lung cancer cells by reactive oxygen species-dependent mitochondrial dysfunction and Bim induction. Int J Oncol 2014;45:1769-77.
30. Hwang KE, Kim YS, Hwang YR, Kwon SJ, Park DS, Cha BK, *et al*. Pemetrexed induces apoptosis in malignant mesothelioma and lung cancer cells through activation of reactive oxygen species and inhibition of sirtuin 1. Oncol Rep 2015;33:2411-9.
31. Muroya M, Chang K, Uchida K, Bougaki M, Yamada Y. Analysis of cytotoxicity induced by proinflammatory cytokines in the human alveolar epithelial cell line A549. Biosci Trends 2012;6:70-80.
32. Ahamed M. Silica nanoparticles-induced cytotoxicity, oxidative stress and apoptosis in cultured A431 and A549 cells. Hum Exp Toxicol 2013;32:186-95.
33. Tang Y, Shen Y, Huang L, Lv G, Lei C, Fan X, *et al*. *In vitro* cytotoxicity of gold nanorods in A549 cells. Environ Toxicol Pharmacol 2015;39:871-8.
34. De-Ugarte L, Balcells S, Guerri-Fernandez R, Grinberg D, Diez-Perez A, Nogues X, *et al*. Effect of the tumor suppressor miR-320a on viability and functionality of human osteosarcoma cell lines compared to primary osteoblasts. Appl Sci 2020;10:2852.
35. Zhao W, Sun Q, Yu Z, Mao S, Jin Y, Li J, *et al*. MiR-320a-3p/ELF3 axis regulates cell metastasis and invasion in non-small cell lung cancer via PI3K/Akt pathway. Gene 2018;670:31-7.
36. Khandelwal A, Sharma U, Barwal TS, Seam RK, Gupta M, Rana MK, *et al*. Circulating miR-320a acts as a tumor suppressor and prognostic factor in non-small cell lung cancer. Front Oncol 2021;11:645475.
37. Shoshan-Barmatz V, De Pinto V, Zweckstetter M, Raviv Z, Keinan N, Arbel N. VDAC, a multi-functional mitochondrial protein regulating cell life and death. Mol Aspects Med 2010;31:227-85.
38. Zhang G, Jiang G, Wang C, Zhong K, Zhang J, Xue Q, *et al*. Decreased expression of microRNA-320a promotes proliferation and invasion of non-small cell lung cancer cells by increasing VDAC1 expression. Oncotarget 2016;7:49470-80.